

## Basic Science and Experimental Studies

# Severe Mechanical Dyssynchrony Causes Regional Hibernation-Like Changes in Pigs With Nonischemic Heart Failure

VINCENZO LIONETTI, MD, PhD,<sup>1,2,\*</sup> GIOVANNI D AQUARO, MD,<sup>3,\*</sup> ANCA SIMIONIUC, MD,<sup>1</sup> CLAUDIO DI CRISTOFANO, MD,<sup>7</sup> FRANCESCA FORINI, PhD,<sup>3</sup> FEDERICA CECCHETTI, PhD,<sup>5</sup> MANUELA CAMPAN, MD,<sup>1</sup> DANIELE DE MARCHI, BSc,<sup>3</sup> FABIO BERNINI, BSc,<sup>1</sup> MARIA GRANA, MD,<sup>6</sup> MONICA NANNIPIERI, MD,<sup>5</sup> MASSIMILIANO MANCINI, MD,<sup>7</sup> MASSIMO LOMBARDI, MD,<sup>3</sup> FABIO A RECCHIA, MD, PhD,<sup>1,4</sup> AND ALESSANDRO PINGITORE, MD, PhD<sup>3</sup>

*Pisa, Italy; Bologna, Italy; Pisa, Italy; Valhalla, New York; Latina, Italy*

## ABSTRACT

**Background:** Sustained left ventricular (LV) dyssynchrony can lead to heart failure (HF) in the absence of coronary artery stenosis. We tested whether myocardial hibernation underlies the LV functional impairment caused by high-frequency pacing, an established model of nonischemic dilated cardiomyopathy.

**Methods and Results:** Regional LV contractile and perfusion reserve were assessed by magnetic resonance imaging, respectively, as end-systolic wall thickening (LVESWT) and myocardial perfusion reserve index (MPRI) at rest and during low-dose dobutamine stress (LDDS, 10  $\mu\text{g}\cdot\text{kg}\cdot\text{min}$  intravenously for 10 minutes) in failing minipigs ( $n = 8$ ). LV tissue was analyzed for glycogen deposits and other molecular hallmarks of hibernation. LDDS caused a marked increase in LVESWT ( $27 \pm 2.98$  vs.  $7.15 \pm 3\%$ ,  $P < .05$ ) and MPRI ( $2.1 \pm 0.5$  vs.  $1.3 \pm 0.3$ ,  $P < .05$ ) in the region that was activated first (pacing site) compared with the opposite region. Myocardial glycogen content was markedly increased in the pacing site ( $P < .05$  vs. opposite region). In addition, gene expression of glycogen phosphorylase was reduced in pacing site compared with opposite regions ( $0.71 \pm 0.1$  vs.  $1.03 \pm 0.3$ ,  $P < .05$ ), whereas that of hexokinase type II was globally reduced by 83%.

**Conclusions:** The combination of high heart rate and sustained dyssynchronous LV contraction causes asymmetrical myocardial hibernation, in absence of coronary artery stenosis. (*J Cardiac Fail* 2009;15:920–928)

**Key Words:** Low-dose dobutamine, MRI, dilated cardiomyopathy, pacing.

From the <sup>1</sup>Sector of Medicine, Scuola Superiore Sant'Anna, Pisa, Italy; <sup>2</sup>National Institute of Biostructures and Biosystems, Bologna, Italy; <sup>3</sup>Institute of Clinical Physiology, CNR-Fondazione G. Monasterio, Pisa, Italy; <sup>4</sup>Department of Physiology, New York Medical College, Valhalla, 10595, USA; <sup>5</sup>Department of Internal Medicine, University of Pisa, Italy; <sup>6</sup>Unit of Anesthesiology and Intensive Care Medicine, Department of General Surgery, Vascular Surgery and Transplants, Cisanello Hospital, Pisa, Italy and <sup>7</sup>Department of Experimental Medicine, Sapienza University of Roma, Polo Pontino, I.C.O.T., Latina, Italy.

Manuscript received March 31, 2009; revised manuscript received June 4, 2009; revised manuscript accepted June 8, 2009.

Reprint requests: Alessandro Pingitore, MD, PhD, Institute of Clinical Physiology-CNR, Via G. Moruzzi n. 1, 56122 Pisa, Italy. E-mail: pingi@ifc.cnr.it

\*These authors have equally contributed to this work.

F.A. Recchia is an Established Investigator of the American Heart Association.

Supported by the Compagnia di San Paolo, Torino, Italy, and by intramural funds of the Institute of Clinical Physiology, CNR-Fondazione G. Monasterio, Pisa, Italy.

Conflict of Interest: none

1071-9164/\$ - see front matter

© 2009 Elsevier Inc. All rights reserved.

doi:10.1016/j.cardfail.2009.06.436

Nonischemic dilated cardiomyopathy (DCM) is defined as severe ventricular dysfunction in the absence of angiographically detectable coronary alterations.<sup>1</sup> Despite this classical definition, patients with idiopathic DCM display marked myocardial blood flow abnormalities characterized by higher glucose uptake and impaired vasodilatory response to metabolic and pharmacological stimuli.<sup>2-4</sup> One of the potential consequences of this functional impairment is an inadequate oxygen supply to stressed cardiac regions. Consistently, we have recently shown that cardiac lactate output markedly increases in DCM patients subjected to moderate pacing stress, indicating a more active anaerobic glycolysis.<sup>5</sup> Therefore, it is conceivable that repetitive, albeit silent, episodes of regional ischemia triggered by stress and oxygen demand/supply mismatch in DCM lead to myocardial damage, which in turn affects cardiac performance and triggers a vicious cycle. This “microvascular ischemic hypothesis” is further supported by the negative prognostic significance of

depressed myocardial blood flow in idiopathic left ventricular (LV) dysfunction,<sup>6</sup> yet in the absence of more direct evidences, it remains debated.

Pacing-induced heart failure (HF) mimics many of the pathophysiological and molecular features of clinical DCM<sup>7</sup> and is well suited to perform combined in vivo and ex vivo measurements and assays.<sup>8</sup> Our model of LV tachypacing is characterized by dyssynchronous contraction and asymmetric functional abnormalities,<sup>9</sup> similar to those commonly found in a large number of HF patients.<sup>10-12</sup> Notably, as shown by other authors and by us,<sup>9,11</sup> after a few weeks of incessant high-frequency pacing basal and stimulated myocardial perfusion is markedly impaired, especially in regions with more pronounced contractile derangement, such as in patients with DCM.<sup>3-5,12</sup> Therefore chronic tachypacing may amplify the combination of high-energy demand and inadequate blood delivery proposed by some authors as a major pathogenic mechanism for human DCM. Based on these premises, the present study tested the hypothesis that sustained high-frequency pacing causes areas of ventricular hibernation (ie, contractile downgrading of viable myocardium aimed at minimizing energy requirements and preventing irreversible tissue damage).<sup>13</sup>

In vivo studies were performed using cardiac magnetic resonance imaging (MRI) combined with low-dose dobutamine stress (LDDS), a method that recently proved very efficacious to detect regional myocardial viability in ischemic and idiopathic DCM patients.<sup>14,15</sup> In vivo regional measurements were followed by myocardial tissue analysis of corresponding segments to determine histological and biochemical hallmarks of hibernation.

## Materials and Methods

### Animal Preparation

Eight male, sexually mature minipigs (35 to 40 kg) were sedated with a cocktail of tiletamine hydrochloride and zolazepam hydrochloride (8 mg/kg<sup>-1</sup> intramuscularly) and premedicated with atropine sulfate (0.1 mg/kg<sup>-1</sup> intramuscularly). General anaesthesia was subsequently induced with propofol (2-4 mg/kg<sup>-1</sup> intravenously) and maintained with 1% to 2% isoflurane in 60% air and 40% oxygen. The pigs were chronically instrumented as previously described.<sup>9</sup> Briefly, a catheter was surgically inserted in the descending thoracic aorta, a solid-state pressure gauge (Konigsberg Instruments) into the left ventricle through the apex, and a screw-type unipolar, epicardial-pacing lead (5071 IS-1 UNI; Medtronic, Inc) was attached to the left ventricular (LV) free wall, approximately 3 cm distal to the atrioventricular margin. A programmable pacemaker (PREVAIL, Medtronic, Inc) was implanted in a subcutaneous pocket. Antibiotics were given after surgery, and the pigs were allowed to fully recover. This investigation was approved by the Animal Care Committee of the Italian Ministry of Health and was in accordance with the Italian law (DL-116, Jan. 27, 1992), which is conformed to the *Guide for the Care and Use of Laboratory Animals* published by the US National Institutes of Health (NIH Publication No. 85-23, revised 1996).

### Experimental Protocol

HF was induced by pacing the left ventricle at 180 beats/min for 3 weeks as previously described.<sup>9</sup> After this pacing time, LV end-diastolic pressure was ~20 mm Hg, which corresponded to severe HF. We chose not to wait for decompensate HF, because at that terminal stage, the animals would have not tolerated long MRI procedures. Diagnostic imaging was performed, after overnight fasting, in minipigs sedated with continuous infusion of midazolam (0.1 mg kg<sup>-1</sup>·h<sup>-1</sup> intravenously) at spontaneous breathing, as previously described.<sup>9</sup> Hemodynamics and MRI measurements were performed before pacing the left ventricle (control) and in the failing heart. The experiments were performed at spontaneous heart rate, with the pacemaker turned off, and during LDDS at a single dose induced by infusing 10 µg min<sup>-1</sup>·kg<sup>-1</sup> of dobutamine,<sup>16,17</sup> a well-established method to study contractile and perfusion reserve in humans<sup>18</sup> and in experimental animals.<sup>19</sup> Eight additional, healthy adult male sham-operated minipigs were sacrificed to collect normal cardiac tissue samples for histological and molecular analysis (normal hearts).

### Hemodynamic Recordings

The aortic catheter was attached to a strain-gauge transducer to measure pressure and LV pressure was measured using the solid-state pressure gauge. All analogic signals were recorded and stored in computer memory through an analog-digital interface (National Instruments), at a sampling rate of 250 Hz for later analysis.

### Cardiac MRI

Regional LV myocardial function at rest and during LDDS was quantified by conventional MRI, as previously described.<sup>9</sup> LV regions close to the site of pacing (ie, the anterior and anterolateral) were named “pacing site” and those remote to the pacing site (ie, the inferior and septal-inferior) were named “opposite site.”

### Global LV Function

Cine-MRI images were acquired with a 1.5 Tesla MRI scanner (Signa Excite HD, GE Medical Systems, Waukesha, WI), maximal gradient intensity 50 mT/m, slew rate 150 T·m·s, using a non-breath-hold electrocardiogram-gated, steady-state free precession pulse sequence, as previously described.<sup>9</sup>

### Regional LV Contractile Function

Regional LV contractile function was assessed as previously described.<sup>9</sup> Briefly, we determined the end-systolic LV wall thickening at rest and during LDDS in 3 short-axis segments. The slices located between atrioventricular plane and papillary muscles were defined as “basal,” those at papillary level were defined as “middle” and those below papillary insertion were defined as “apical.” The assessment of regional LV thickening at rest and during LDDS allows quantifying the ventricular contractile reserve.<sup>14,20</sup> Clinical and experimental studies have clearly shown that the presence of contractile reserve during inotropic stimulation, assessed as end-systolic wall thickening, is highly specific for myocardial viability<sup>21</sup> and hibernation.<sup>22</sup>

### Myocardial Perfusion

Myocardial perfusion at rest and during LDDS was assessed with the first-pass technique, as previously described.<sup>9,23,24</sup> The relative upslope of signal intensity (myocardial upslope divided

**Table 1.** Hemodynamic and Global Contractile Function

	Control	Control + LDDS	HF	HF + LDDS
HR, beats/min (n = 8)	85.4 ± 2.43	124.85 ± 2.2 <sup>†</sup>	115.28 ± 2.3*	136 ± 2 <sup>†</sup>
MAP, mmHg (n = 8)	105.28 ± 8.8	93.4 ± 3.92 <sup>†</sup>	82.02 ± 7.53*	78.57 ± 4.62*
DP, mmHg x beats/min (n = 8)	9070.66 ± 685	11,576.63 ± 650.39	8560.43 ± 690	10,620 ± 1041
LVEDV, mL (n = 8)	62.3 ± 3.2	54.57 ± 4.7 <sup>†</sup>	83.72 ± 10.4*	66.92 ± 7.89 <sup>†</sup>
LVESV, mL (n = 8)	15 ± 1.78	11.28 ± 1.85	49.05 ± 9*	28.9 ± 5.37* <sup>†</sup>
EF, % (n = 8)	77 ± 1.78	76.85 ± 2.12	38.14 ± 3.5*	50.3 ± 6.4* <sup>†</sup>
SVR, (dynes*sec)/cm <sup>-5</sup> (n = 8)	1923 ± 93	1348 ± 159.4	1743.36 ± 359.33	1247.14 ± 159.73

HF, heart failure; LDDS, low-dose dobutamine stress; HR, heart rate; MAP, mean arterial pressure; DP, double product; LVEDV, left ventricle end diastolic volume; LVESV, left ventricle end-systolic volume; EF, ejection fraction; SVR, systemic vascular resistance.

\**P* < .05 vs. control.

<sup>†</sup>*P* < .05 vs. rest at the same time point.

LV cavity upslope) for each myocardial segment was obtained at rest and during dobutamine infusion. The myocardial perfusion reserve index (MPRI) was calculated as the ratio between indexed upslope at rest and during LDDS in each myocardial segment. The MPRI by first-pass contrast MRI is an established method to evaluate the regional distribution of the perfusion reserve,<sup>23</sup> and its accuracy in assessing myocardial stress perfusion by LDDS has been validated previously.<sup>25</sup>

### Regional Wall Stress

Regional end-systolic LV wall stress was assessed in the basal and middle regions of pacing and opposite sites related to the LV displacement during the cardiac cycle. We employed the method established by Balzer et al and in part modified by us.<sup>9</sup>

### Myocardial Fibrosis

To assess for the presence of tissue fibrosis, gadolinium delayed contrast-enhanced images were acquired in 2-dimensional segmented

inversion-recovery-prepared gradient-echo sequence 10 minutes after administration of contrast agent Gd-DTPA (0.2 mmol/kg<sup>-1</sup>, intravenously) in short axis views, as previously described.<sup>9</sup>

### Histological Analysis

Transmural tissue samples were taken from LV pacing and opposite sites. The samples were immediately fixed for at least 48 hours in 10% formalin. Five-micron thick paraffin embedded sections were stained using hematoxylin and eosin. Myocyte glycogen content, a hallmark of hibernation<sup>26,27</sup> was assessed from the periodic acid-Schiff (PAS) stained sections by 2 independent observers blinded to the origin of the specimen. The myocyte glycogen contents and interstitial fibrous tissues was quantitatively evaluated capturing 10 random fields images at 10 magnification (3.0 megapixel resolution), and analyzed by using an automatic image analyzer (Metamorph vers. 6.2).<sup>28</sup> PAS diastase was performed on an adjacent section followed by PAS staining to confirm that the PAS positive material was glycogen.

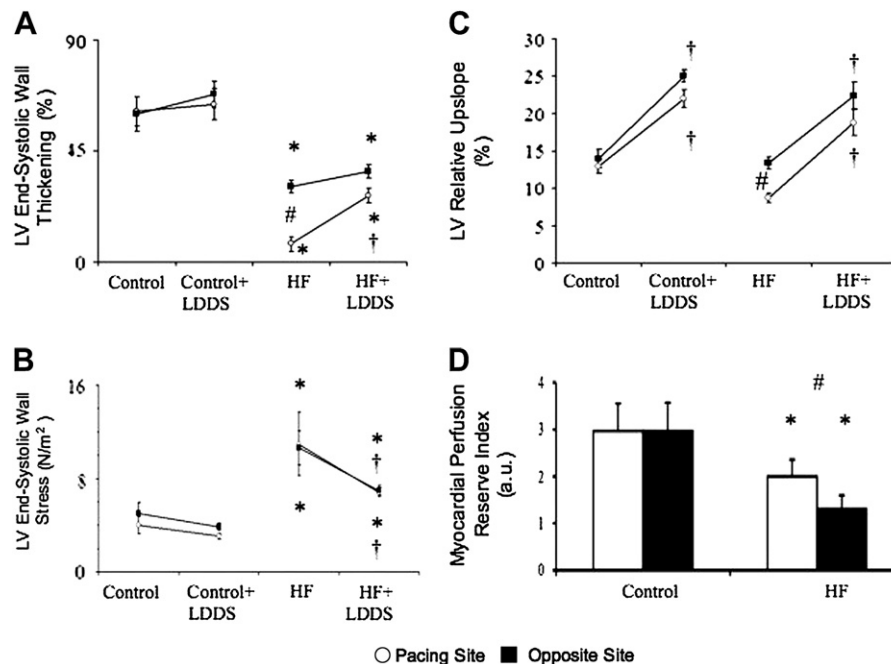


**Fig. 1.** Cardiac magnetic resonance imaging (MRI) regional measurements at rest and during low-dose dobutamine stress (LDDS). (A) Regional changes in left ventricular (LV) end-systolic wall thickening. (B) Regional changes in LV end-systolic wall stress. (C) Mean values for regional LV relative upslope. (D) Changes in regional myocardial perfusion reserve index. n = 8. \**P* < .05 vs. the corresponding experimental condition before pacing (control). <sup>†</sup>*P* < .05 vs. rest at the same time point. #*P* < .05 pacing site vs. opposite site.

Histochemical analysis, Masson's trichomic, and Sirius red were used to assess the interstitial fibrous tissue. Morphological analysis was used for interstitial inflammatory cells and blood vessels using an  $11 \times 11$  graticule.<sup>27</sup>

### Mitochondrial Protein Isolation

Mitochondrial proteins were extracted from frozen cardiac muscle tissue by means of a mitochondrial isolation kit (MITO-ISO1, Sigma), as previously described.<sup>29</sup>

### Enzymatic Activities

The activity of the cytochrome c oxidase and citrate synthase in extracted mitochondria were respectively measured by means of a colorimetric cytochrome C oxidase assay kit (CYTOCOX1, Sigma) and citrate synthase assay kit (CS0720, Sigma) according to the manufacturer's instruction, as previously described.<sup>30</sup>

### Western Blot Assay

Protein was extracted from frozen tissue as previously described.<sup>31</sup> Fifty microgram of total protein was resolved by sodium dodecyl sulfate polyacrylamide gel electrophoresis on 15.0% gel and blotted electrophoretically. Thereafter, the membrane was probed with specific antibody against heat shock protein-70 (HSP-70, dilution 1:100, Santa Cruz Biotechnology) and hypoxia-inducible factor-1 $\alpha$  (HIF-1 $\alpha$ , dilution 1:1000, Santa Cruz Biotechnology). After probing with the secondary peroxidase-conjugated antibody, the protein bands were developed in a chemiluminescence substrate solution (Pierce SuperSignal Chemiluminescents Substrate) and then reprobbed for beta-actin (dilution 1:1000, Santa Cruz Biotechnology) to verify the uniformity of protein loading.

### Gene Expression Analysis

RNA was extracted from cardiac tissue sample (50 to 100 mg), immediately placed in ice-cold RNeasy lysis buffer (Qiagen, Milan, Italy) and stored at  $-80^{\circ}\text{C}$  using standard methods and analyzed using reverse transcription followed by real-time quantitative polymerase chain reaction for the transcripts of interest, as described previously.<sup>31,32</sup> Analysis was focused on the traditional housekeeping genes glyceraldehyde-3-phosphate dehydrogenase and ribosomal 18S (18S) on the glycogen-related key genes, glycogen phosphorylase (PYGM), glycogen synthase 1 (GYS1), and hexokinase 2 (HK-2). Specific quantitative assays were designed from swine sequences available in GenBank.

### Statistics

Data are presented as mean  $\pm$  standard error of the mean. Statistical analysis was performed by employing commercially available software (SPSS for Windows, version 11.1; SPSS Inc, Chicago, IL). Myocardial perfusion, contractility, and wall stress changes at different time points in the pacing group were compared by 1- and, for differences between cardiac regions, 2-way analysis of variance followed by the Bonferroni post-hoc test. Histological and molecular differences between failing hearts and normal hearts were assessed by *t*-test or with 2-way analysis of variance when different regions were compared. Correlations between groups of values were evaluated calculating the best fit, based on least-squares regression analysis. For all the statistical analyses, significance was accepted at  $P < .05$ .

## Results

### Hemodynamic and LV Global Function

LV end-diastolic pressure was  $5.7 \pm 1.0$  mmHg at control and increased up to  $20.1 \pm 4.1$  mmHg after 21 days of

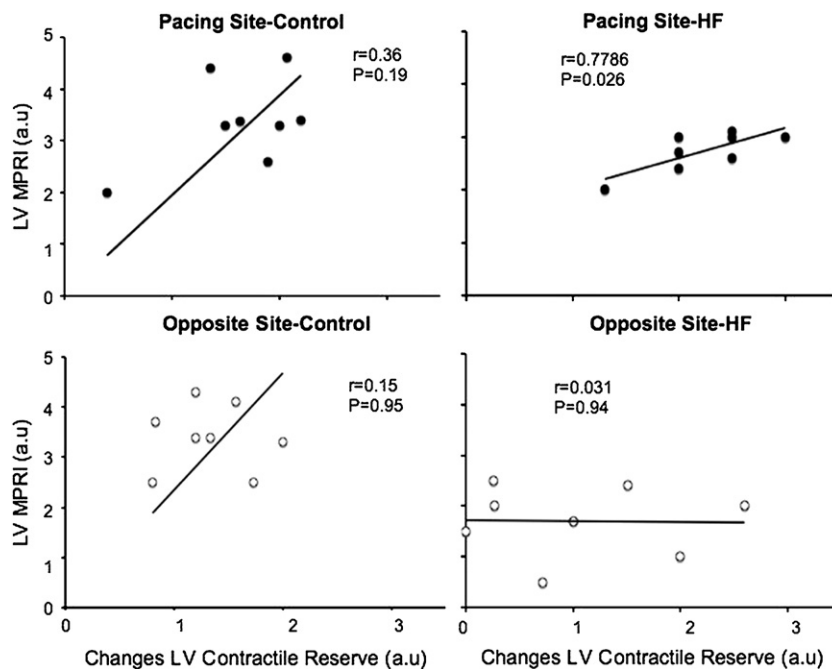


**Fig. 2.** Correlations between changes in left ventricular (LV) myocardial perfusion reserve index (MPRI) and in end-systolic LV wall thickening induced by low-dose dobutamine stress (LDDs). Changes in wall thickening occurring during LDDs are normalized to baseline values.

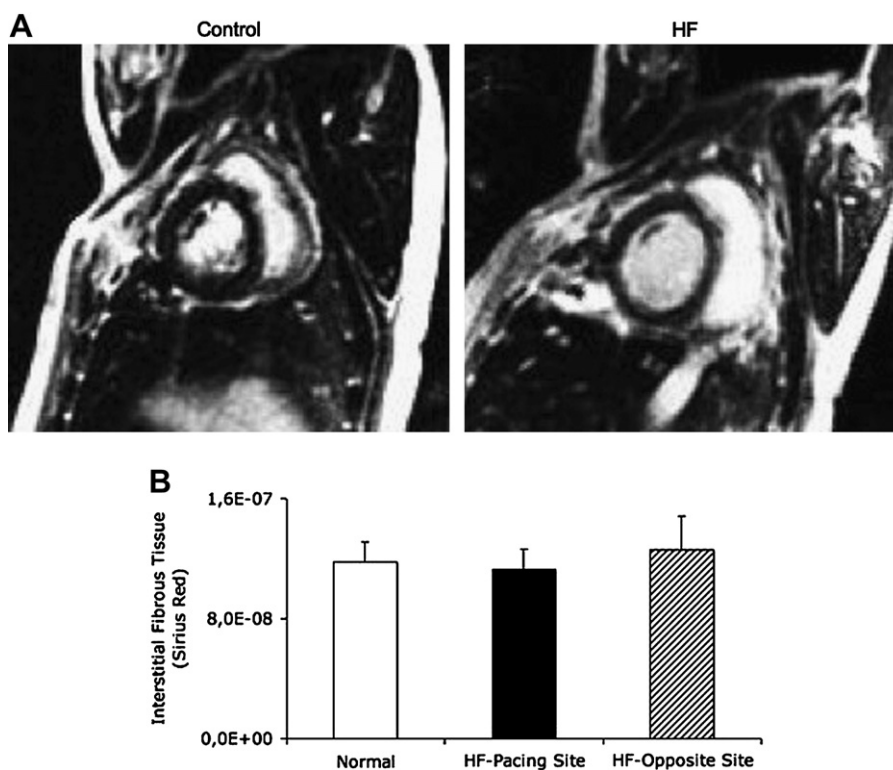


**Fig. 3.** Myocardial fibrosis. (A) Representative images of gadolinium delayed contrast enhancement magnetic resonance imaging (MRI) from a heart studied before starting the pacing protocol (control) and in failure (heart failure [HF]). (B) Regional interstitial fibrous tissue measured quantitatively from the Sirius red stained sections in normal and failing left ventricle.  $n = 8$  per group.

continuous pacing ( $P < .05$ ), but pigs were not in end-stage failure. Table 1 shows changes in hemodynamic and cardiac volumes in response to LDDS at control and HF. LDDS caused a significant increase in heart rate both at control and HF, whereas it is significantly reduced mean arterial pressure only at control. Ejection fraction increased significantly, whereas systemic vascular resistance, which did not change significantly in HF compared with control as found by other authors in the pacing model,<sup>33</sup> was not significantly affected by LDDS. On the other hand, dobutamine infusion reduced significantly the end-diastolic volume both at control and HF. Interestingly, the double product, an indirect measure of oxygen consumption,<sup>17</sup> did not change significantly during dobutamine stimulation.

### Regional LV Wall Thickening

The regional contractile response to LDDS is shown in (Fig. 1A). Dobutamine induced a significant improvement in LV wall thickening, an index of regional contractile function, in the pacing site. Conversely, there was no significant increase of contractility in the opposite site.

### Regional LV End-systolic Wall Stress

The end-systolic wall stress was significantly increased in both LV regions after 21 days of pacing, compared with control, by  $50 \pm 8.54\%$ . During LDDS, the end-systolic wall stress was significantly reduced in both LV sites of failing heart by approximately 37% (Fig. 1B).

### Regional LV Myocardial Perfusion and Viability

After 21 days of pacing, the upslope was lower in the pacing site, indicating a significant relative hypoperfusion and significantly enhanced in both LV sites by LDDS (Fig. 1C). However, as shown in Fig. 1D, MPRI was significantly increased in the pacing site compared with the opposite site, indicating a marked and asymmetric improvement of myocardial perfusion. As shown in Fig. 2, only in HF there was a direct and significant correlation between changes in MPRI and in end-systolic LV wall thickening in response to LDDS; this was limited to the pacing site. On the other hand, no significant correlation was found between LDDS-induced changes in MPRI and wall stress (data not shown). To test whether regional differences in function and flow could be due to asymmetric tissue damage and fibrosis, we examined gadolinium-delayed enhancement and found no changes in HF compared with control and no differences between LV pacing and opposite sites (Fig. 3).

### Histological Analysis

No changes in fibrous tissue content (Fig. 3) or in inflammatory cells infiltration (data not shown) were found in HF compared with normal. On the other hand, PAS staining revealed the presence of nonhomogeneous glycogen accumulation in a large fraction of myocytes from the pacing site (Fig. 4), whereas this alteration was seen to a much lesser extent in opposite site.

## Regional Regulation of Survival Proteins

HIF1- $\alpha$ , switch mediator in the metabolic and functional adaptation to chronic anaerobic conditions,<sup>34</sup> and HSP70, cytoprotective HSP in response to ATP depletion,<sup>35</sup> were measured by Western blot analysis. As shown in Fig. 5A, the expression of HIF1- $\alpha$  was significantly increased in the pacing site of the failing myocardium compared with the opposite regions and to normal myocardium, whereas HSP70 levels were increased in pacing site compared with normal heart, but higher in the opposite regions (Fig. 5B).

## Enzymatic Activities and Gene Expression

The activity of citrate synthase was significantly reduced in mitochondria isolated from the myocardium of the opposite region compared with pacing site and to normal heart (Fig. 6A). However, the cytochrome oxidase activity, corrected by the citrate synthase activity, was not significantly changed in both failing regions (Fig. 6B). Compared with normal, the PYGM was significantly downregulated in the pacing site of failing heart, in presence of a global downregulation of myocardial HK-2 and GYS1 (Fig. 7). Gene expression alterations were observed whether mRNA values were expressed relative to the housekeeping glyceraldehyde-3-phosphate dehydrogenase or to ribosomal 18S content.

## Discussion

After 21 days of sustained, high-frequency mechanical dyssynchrony induced by pacing the LV free wall, MRI at spontaneous heart rate revealed a regional hibernating-like response during LDDS: both perfusion and contractile reserve were higher in the LV pacing site, despite a uniform decrease of the systolic ventricular wall stress and maintained regional dyssynchronous contraction. Conversely, the opposite site, with a better myocardial function at rest, displayed no significant changes in contractility and a reduced myocardial perfusion reserve during LDDS. Moreover, flow and contractile reserves during LDDS were directly correlated in the pacing site: this finding is relevant if we consider that a prerequisite for myocardial hibernation is the maintenance of flow/function relationship in the presence of reduced myocardial blood flow.<sup>36</sup>

Our functional findings are strongly supported by histological evidence of patchy glycogen deposits in cardiomyocytes from the LV region with hibernation-like response to LDDS (ie, the pacing site). As previously described by other authors, this alteration is characteristic of hibernated myocardium.<sup>27</sup> Nikolaidis et al<sup>28</sup> have shown an increase in glycogen content in the failing myocardium of chronically paced dogs. We show now that glycogen accumulation is not uniform, but displays a patchy distribution in LV myocardium of the regions activated early (pacing site) in the absence of fibrosis. The regional correspondence

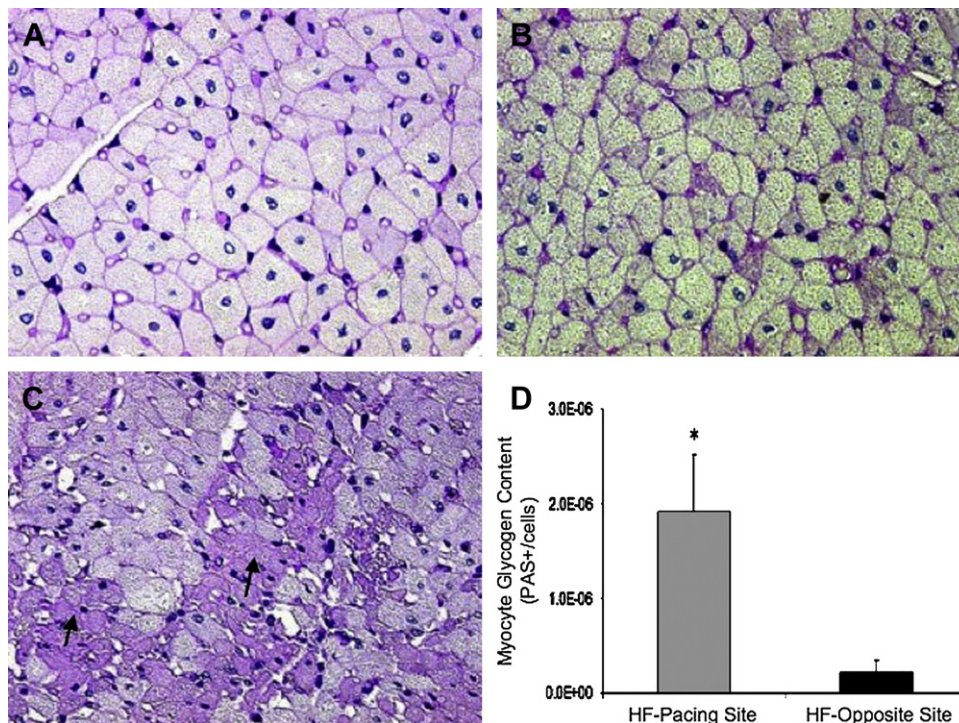


**Fig. 4.** Histological sections of the left ventricular (LV) myocardium stained with periodic acid–Schiff reagent (PAS). (A) Myocardium from normal left ventricle; (B) myocardium from opposite site of failing left ventricle; (C) myocardium obtained from the pacing site of failing left ventricle; (D) regional myocardial glycogen contents (black arrows) measured quantitatively from the PAS-stained sections.  $n = 8$  per group.  $*P < .05$  vs. opposite regions at 21 days.

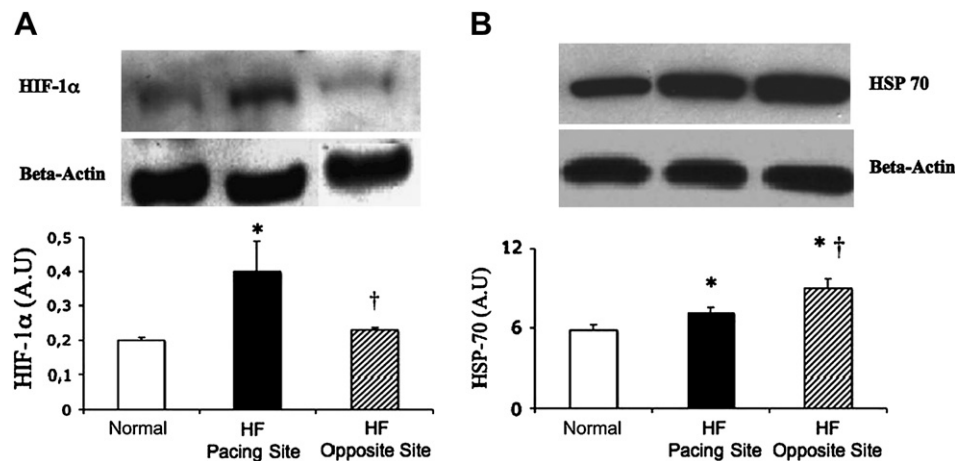


**Fig. 5.** Regional HIF1- $\alpha$  (A) and HSP-70 (B) expression in left ventricle of normal (n = 6) and failing hearts (n = 6). \* $P < .05$  vs. normal heart (normal). † $P < .05$  pacing site vs. opposite site.

between increased glycogen content and higher myocardial functional reserve is consistent with the development of hibernation in areas with worse perfusion-contraction coupling. Although our results are limited to an experimental model of disease, they nevertheless support the concept that severe mechanical dyssynchrony, in the absence of coronary stenosis, leads to hibernation in the region that is activated first.

The molecular mechanisms leading to myocardial hibernation are very complex and in our in vivo model we selected only some molecular candidates. First, we measured protein expression of HIF1- $\alpha$ , whose important role in myocardial hibernation has been well documented.<sup>34</sup> Consistent with both of functional and histological alterations, HIF1- $\alpha$  protein expression was markedly increased in the pacing site, but not in the opposite region. Second, we measured protein levels of HSP70, a recognized cytoprotective factor that increases in response to cellular ATP-depletion<sup>37</sup> and mechanical stretch.<sup>38</sup> HSP70 level was significantly increased in the pacing site compared with normal myocardium, consistent with energy sparing in hibernated myocardium. Surprisingly, myocardial expression of HSP70 was more increased in the opposite site, which is still contracting in presence of a significant reduction of the citrate synthase activity. This novel finding is suggestive for a higher ATP consumption and mechanical activity in the opposite region of failing heart. Thus, in presence of a global increased LV glucose uptake and end-systolic wall stress,<sup>9</sup> it is conceivable that high-rate dyssynchrony induces hibernation by modulating regional energy turnover and metabolic activity after reduction of myocardial perfusion. The increased glycogen storage in myocytes hibernated plays a key role in protection.<sup>26,39</sup> In our animal model, we measured the cardiac gene expression of HK-2, which is responsible for glucose phosphorylation,<sup>40</sup> PYGM and GYS1, the 2 enzymes controlling glycogen synthetic rates. We found that PYGM is markedly downregulated only in the pacing site despite a global decrease in LV HK-2 and GYS1.

Although we could not determine activity of these enzymes, our novel data strongly suggest that severe and prolonged mechanical dyssynchrony involves downregulation of the glycogen degradation pathway in the less perfused cardiac region and therefore explains glycogen accumulation in the pacing site. Our results even support the conclusions of a recent report on the cytoprotective role of glycogen breakdown suppression in ischemic heart.<sup>41</sup> We cannot exclude that a dyssynchronous mechanical stimulation of cardiomyocytes may serve, at transcriptional level,

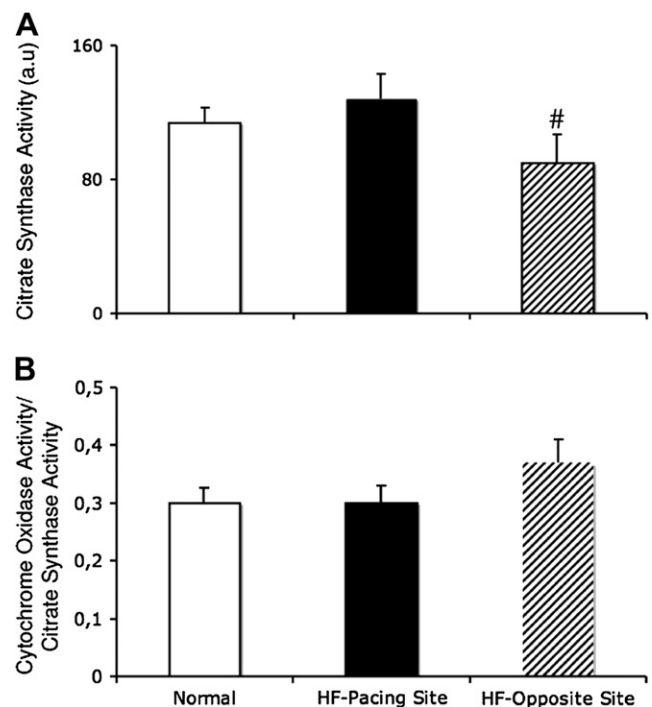


**Fig. 6.** Regional changes of enzymatic activities in mitochondria extracted from left ventricle of normal (n = 6) and failing hearts (n = 6): (A) citrate synthase activity; (B) cytochrome oxidase activity expressed as a ratio with the citrate synthase activity. # $P < .05$  pacing site vs. opposite site.

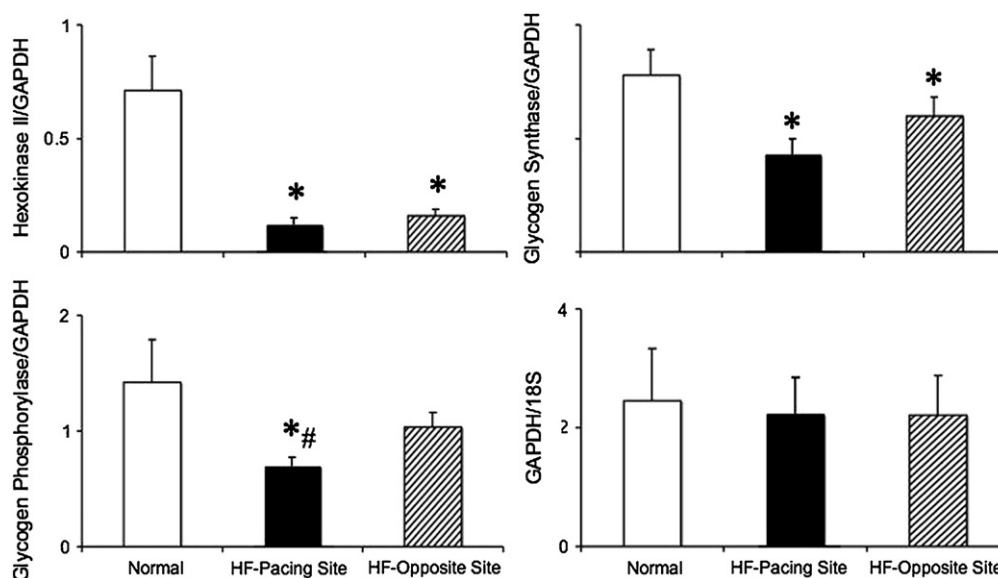


**Fig. 7.** Messenger RNA levels in left ventricular myocardium from normal ( $n = 6$ ) and failing heart ( $n = 6$ ) normalized to the housekeeping glyceraldehyde-3-phosphate dehydrogenase (GAPDH) or 18S, and expressed as a ratio (arbitrary units). \* $P < .05$  vs. normal heart (normal). # $P < .05$  pacing site vs. opposite site.

as important determinant of regional myocyte expression of enzymes that control glycogen turnover<sup>42</sup> and priming some long-term adaptive effects from a sustained metabolic demand/supply mismatch.

A better understanding of this concept could be of clinical importance to expand conditions of functional salvage of the dyssynchronous failing myocardium. Our findings may prompt future investigations to better decipher the adaptive mechanisms triggered by dyssynchronous contraction in the progression of non ischemic HF.

In conclusion, we showed that, even in the absence of coronary stenosis, the combination of prolonged hypoperfusion and severe dyssynchronous LV contraction is sufficient to cause regional hibernating-like adaptive mechanisms by modulating the expression of glycogen phosphorylase in the region that is activated first. Our results also suggest the possibility that the pacing model recapitulates a long-term adaptive phenomenon possibly occurring in human DCM.

### Acknowledgments

We are grateful to Silvia Burchielli, Massimiliano Mancini, Vincenzo Positano, and Barbara Scattini for their excellent technical assistance.

### References

- Jessup M, Bronzena S. Heart failure. *N Engl J Med* 2003;348:2007–18.
- Treasure CB, Vita JA, Cox DA, Fish RD, Gordon JB, Mudge GH, et al. Endothelium dependent dilation of the coronary microvasculature is impaired in dilated cardiomyopathy. *Circulation* 1990;81(3):772–9.
- Neglia D, Parodi O, Gallopin M, Sambuceti G, Giorgetti A, Pratali L, et al. Myocardial blood flow response to pacing tachycardia and to dipyridamole infusion in patients with dilated cardiomyopathy without overt heart failure. A quantitative assessment by positron emission tomography. *Circulation* 1995;92:796–804.
- van den Heuvel AF, van Veldhuisen DJ, van der Wall EE, Blanksma PK, Siebelink HM, Vaalburg WM, et al. Regional myocardial blood flow reserve impairment and metabolic changes suggesting myocardial ischemia in patients with idiopathic dilated cardiomyopathy. *J Am Coll Cardiol* 2000;35:19–28.
- Neglia D, De Caterina A, Marraccini P, Natali A, Ciardetti M, Vecoli C, et al. Impaired myocardial metabolic reserve and substrate selection flexibility during stress in patients with idiopathic dilated cardiomyopathy. *Am J Physiol Heart Circ Physiol* 2007;293:H3270–8.
- Neglia D, Michelassi C, Trivieri MG, Sambuceti G, Giorgetti A, Pratali L, et al. Prognostic role of myocardial blood flow impairment in idiopathic left ventricular dysfunction. *Circulation* 2002;105:186–93.
- Ojaimi C, Qanud K, Hintze TH, Recchia FA. Altered expression of a limited number of genes contributes to cardiac decompensation during chronic ventricular tachypacing in dogs. *Physiol Genom* 2007;29:76–83.
- Recchia FA, Lionetti V. Animal models of dilated cardiomyopathy for translational research. *Vet Res Commun* 2007;31(Suppl 1):35–41.
- Lionetti V, Guiducci L, Simioniu A, Aquaro GD, Simi C, De Marchi D, et al. Mismatch between uniform increase in cardiac glucose uptake and regional contractile dysfunction in pacing-induced heart failure. *Am J Physiol Heart Circ Physiol* 2007;293:H2747–56.
- Kass DA. An epidemic of dyssynchrony: but what does it mean? *J Am Coll Cardiol* 2008;51:12–7.
- Helmer GA, McKirnan MD, Shabetai R, Boss GR, Ross J Jr, Hammond HK. Regional deficits of myocardial blood flow and function in left ventricular pacing induced heart failure. *Circulation* 1996;94:2260–7.
- Skalidis EI, Parthenakis FI, Patrianakos AP, Hamilos MI, Vardas PE. Regional coronary flow and contractile reserve in patients with idiopathic dilated cardiomyopathy. *J Am Coll Cardiol* 2004;44:2027–32.

13. Heusch G, Schulz R, Rahimtoola SH. Myocardial hibernation: a delicate balance. *Am J Physiol Heart Circ Physiol* 2005;288:H984–99.
14. Bree D, Wollmuth JR, Cupps BP, Krock MD, Howells A, Rogers J, et al. Low-dose dobutamine tissue-tagged magnetic resonance imaging with 3-dimensional strain analysis allows assessment of myocardial viability in patients with ischemic cardiomyopathy. *Circulation* 2006;114(1 Suppl):I33–6.
15. Jerosch-Herold M, Sheridan DC, Kushner JD, Nauman D, Burgess D, Dutton D, et al. Cardiac magnetic resonance imaging of myocardial contrast uptake and blood flow in patients affected with idiopathic or familial dilated cardiomyopathy. *Am J Physiol Heart Circ Physiol* 2008;295:H1234–42.
16. Baer FM, Voth E, Schneider CA, Theissen P, Schicha H, Sechtem U. Comparison of low-dose dobutamine-gradient-echo magnetic resonance imaging and positron emission tomography with [18F]fluorodeoxyglucose in patients with chronic coronary artery disease. A functional and morphological approach to the detection of residual myocardial viability. *Circulation* 1995;91:1006–15.
17. Kasama S, Toyama T, Kumakura H, Takayama Y, Ichikawa S, Tange S, et al. Dobutamine stress 99mTc-tetrofosmin quantitative gated SPECT predicts improvement of cardiac function after carvedilol treatment in patients with dilated cardiomyopathy. *J Nucl Med* 2004;45:1878–84.
18. Mazzadi AN, Janier MF, Brossier B, André-Fouet X, McFadden E, Revel D, et al. Dobutamine-tagged MRI for inotropic reserve assessment in severe CAD: relationship with PET findings. *Am J Physiol Heart Circ Physiol* 2004;286:H1946–53.
19. Chin BB, Esposito G, Kraitchman DL. Myocardial contractile reserve and perfusion defect severity with rest and stress dobutamine 99mTc-Sestamibi SPECT in canine stunning and subendocardial infarction. *J Nucl Med* 2002;43:540–50.
20. Banas M, Baldwa S, Suzuki G, Canty JM, Fallavollita JA. Determinants of contractile reserve in viable, chronically dysfunctional myocardium. *Am J Physiol Heart Circ Physiol* 2007;292:H2791–7.
21. Bax JJ, Wijns W, Cornel JH, Visser FC, Boersma E, Fioretti PM. Accuracy of currently available techniques for prediction of functional recovery after revascularization in patients with left ventricular dysfunction due to chronic coronary artery disease: comparison of pooled data. *J Am Coll Cardiol* 1997;30:1451–60.
22. McFalls EO, Kelly RF, Hu Q, Mansoor A, Lee J, Kuskowski M, et al. The energetic state within hibernating myocardium is normal during dobutamine despite inhibition of ATP-dependent potassium channel opening with glibenclamide. *Am J Physiol Heart Circ Physiol* 2007;293:H2945–51.
23. Positano V, Pingitore A, Scattini B, Santarelli MF, De Marchi D, Favilli B, et al. Myocardial perfusion by first pass contrast magnetic resonance: a robust method for quantitative regional assessment of perfusion reserve index. *Heart* 2006;92:689–90.
24. Pingitore A, Lombardi M, Scattini B, De Marchi D, Aquaro GD, Positano V, et al. Head to head comparison between perfusion and function during accelerated high dose dipyridamole magnetic resonance stress for the detection of coronary artery disease. *Am J Cardiol* 2008;101:8–14.
25. Lee DC, Simonetti OP, Harris KR, Holly TA, Judd RM, Wu E, et al. Magnetic resonance versus radionuclide pharmacological stress perfusion imaging for flow limiting stenoses of varying severity. *Circulation* 2004;110:58–65.
26. Kim SJ, Peppas A, Hong SK, Yang G, Huang Y, Diaz G, et al. Persistent stunning induces myocardial hibernation and protection: flow/function and metabolic mechanisms. *Circ Res* 2003;92:1233–9.
27. Gunning MG, Kaprielian RR, Pepper J, Pennel DJ, Sheppard MN, Severs NJ, et al. The histology of viable and hibernating myocardium in relation to imaging characteristics. *J Am Coll Cardiol* 2002;39:428–35.
28. Nikolaidis LA, Hentosz T, Doverspike A, Huerbin R, Stolarski C, Shen YT, et al. Mechanisms whereby rapid RV pacing causes LV dysfunction: perfusion contraction matching and NO. *Am J Physiol Heart Circ Physiol* 2001;281:H2270–81.
29. Sharma AK, Dhingra S, Khaper N, Singal PK. Activation of apoptotic processes during transition from hypertrophy to heart failure in guinea pigs. *Am J Physiol Heart Circ Physiol* 2007;293:H1384–90.
30. Morgunov I, Srere PA. Interaction between citrate synthase and malate dehydrogenase. Substrate channeling of oxaloacetate. *J Bio. Chem* 1998;273:2950–4.
31. Lionetti V, Linke A, Chandler MP, Young ME, Penn MS, Gupte S, et al. Carnitine palmityl transferase-I inhibition prevents ventricular remodeling and delays decompensation in pacing-induced heart failure. *Cardiovasc Res* 2005;66:454–61.
32. Del Ry S, Cabiati M, Lionetti V, Emdin M, Recchia FA, Giannessi D. Expression of C-type natriuretic peptide and of its receptor NPR-B in normal and failing heart. *Peptides* 2008;29:2208–15.
33. Kiuchi K, Shannon RP, Sato N, Bigaud M, Lajoie C, Morgan KG, et al. Factors involved in delaying the rise in peripheral resistance in developing heart failure. *Am J Physiol* 1994;267:H211–6.
34. Depre C, Kim SJ, John AS, Huang Y, Rimoldi OE, Pepper JR, et al. Program of cell survival underlying human and experimental hibernating myocardium. *Circ Res* 2004;95:433–40.
35. Wang D, McMillin JB, Bick R, Buja LM. Response of the neonatal rat cardiomyocyte in culture to energy depletion: effects of cytokines, nitric oxide, and heat shock proteins. *Lab Invest* 1996;75:809–18.
36. Schulz R, Rose J, Martin C, Brodde OE, Heusch G. Development of short-term myocardial hibernation. Its limitation by the severity of ischemia and inotropic stimulation. *Circulation* 1993;88:684–95.
37. Kabakov AE, Budagova KR, Latchman DS, Kampinga HH. Stressful preconditioning and HSP70 overexpression attenuate proteotoxicity of cellular ATP depletion. *Am J Physiol Cell Physiol* 2002;283:C521–34.
38. Frank D, Kuhn C, Brors B, Hanselmann C, Lütjens M, Katus HA, et al. Gene expression pattern in biomechanically stretched cardiomyocytes: evidence for a stretch-specific gene program. *Hypertension* 2008;51:309–18.
39. Ofir M, Arad M, Porat E, Freimark D, Chepurko Y, Vidne BA, et al. Increased glycogen stores due to gamma-AMPK overexpression protects against ischemia and reperfusion damage. *Biochem Pharmacol* 2008;75:1482–91.
40. Southworth R, Davey KAB, Warley A, Garlick PB. A reevaluation of the roles of hexokinase I and II in the heart. *Am J Physiol Heart Circ Physiol* 2007;292:H378–86.
41. Ross TW, Treadway JL, Magee WP, Sutt CJ, McPherson RK, Levy CB, et al. Cardioprotective effects of ingliforib, a novel glycogen phosphorylase inhibitor. *Am J Physiol Heart Circ Physiol* 2004;286:H1177–84.
42. Bilchick KC, Saha SK, Mikolajczyk E, Cope L, Ferguson WJ, Yu W, et al. Differential regional gene expression from cardiac dyssynchrony induced by chronic right ventricular free wall pacing in the mouse. *Physiol Genom* 2006;26:109–15.